Climatic Change (2007) 82:113–130
DOI 10.1007/s10584-006-9148-9

Snow cover variability across central Canada (1978–2002) derived from satellite passive microwave data

Michael A. Wulder · Trisalyn A. Nelson · Chris Derksen · David Seemann

Received: 29 November 2004 / Accepted: 12 May 2006 / Published online: 15 February 2007

Abstract Twenty-four winter seasons (1978–2002) of mean February snow water equivalent (SWE) values were analyzed in an exploration of the spatial pattern of temporal variability in snow cover across the non-mountainous interior of Canada. The SWE data were derived from space-borne passive microwave brightness temperatures processed with a land cover-sensitive suite of algorithms. Spatial patterns in the frequency and amount of variability were investigated on an annual basis through comparisons with average trends over all 24 years. Changes in temporal variability through time were also investigated by comparing three eight year time periods to general trends.

Analyses were synthesized at the ecozone scale in order to link results both to potential land cover influences on algorithm performance and climatological variability in SWE. Prairie and northern ecozones were typically found to be the most variable in terms of SWE magnitude. Analyses indicate that non-treed land cover classes are generally more variable than treed classes. The results also indicate that extreme weather events appear to be occurring with increasing consistency in the Prairie and Arctic regions. Discerning climatologically significant variability in the time series, compared to algorithm-related issues can be a challenge, but in an era of eroding surface observing networks the passive microwave time series represents an important resource for monitoring and detecting trends and variability in terrestrial snow cover.

M. A. Wulder (✉) · D. Seemann
Canadian Forest Service (Pacific Forestry Centre), Natural Resources Canada, Victoria, British Columbia, Canada, V8Z 1M5
e-mail: mwulder@nrcan.gc.ca

T. A. Nelson
University of Victoria, Department of Geography, Victoria, British Columbia, Canada, V8W 3P5

C. Derksen
Climate Research Division, Climate Processes Section, Environment Canada, Downsview, Ontario, Canada, M3H 5T4

1 Introduction

1.1 Snow cover/climate

Snow cover is intimately linked with atmospheric circulation and the global climate system (Cohen and Entekhabi 2001; Gong et al. 2003). As such, snow cover is an appropriate indicator of climate perturbations and may be a suitable surrogate for investigations of climate change (Serreze et al. 2000). Variability in terrestrial snow cover has a significant influence on water and energy cycles, as well as socio-economic and environmental repercussions (WCRP 2002). Understanding the spatial pattern in the temporal variability of snow cover may add to the current understanding of global climate change and provide a mechanism for exploring future trends.

The importance of snow cover to climate and hydrological modelling has led to considerable efforts to the accurate representation of snow cover over large areas and long time periods. For instance, from a climatological perspective, snow cover is significant as the high albedo and corresponding low absorption of snow results in decreased maximum daytime temperatures, while a high thermal emissivity and corresponding loss of infrared radiation act to lower daily minimum surface temperatures. The low thermal conductivity of fresh snow traps heat and modifies energy exchanges with the overlying atmosphere, with melting snow acting as a sink for latent heat. From a hydrological perspective, snow acts as the frozen storage term in the water balance, and can undergo redistribution, metamorphism, and phase change (sublimation) before actively entering the water cycle.

Current conventional snow cover measurement networks are sparse, especially at northern latitudes. To accommodate this paucity of ground measurement, various snow cover products are operationally produced from satellite data sources by numerous government agencies in North America using both visible and passive microwave imagery. Identifying snow extent using visible wavelength imagery has been successful (Hall et al. 2002) due to the optically reflective nature of snow cover. There is added value to the use of passive microwave data, as microwave brightness temperatures respond to changes in snow depth and density due to scattering of the microwave signal by snow grains – a relationship that can be exploited to produce estimates of snow water equivalent (SWE) under dry snow conditions. For many hydrological and numerical modelling applications, it is essential to characterize not only where snow cover is (extent) but how much water is stored in the snowpack (SWE).

The space-borne passive microwave time series from the Scanning Multichannel Microwave Radiometer (SMMR, 1978–1987), and Special Sensor Microwave/Imager (SSM/I, 1987 – present) is one of the longest continuous satellite data records available. Passive microwave snow cover algorithm development efforts have been varied, focused upon the retrieval of snow extent (Grody and Basist 1996), snow depth (Chang et al. 1990; Kelly et al. 2003), and SWE (Josberger et al. 1998; Tait 1998; Pulliainen and Hallikainen 2001). While the majority of these efforts have been hemispheric or global in perspective, the Climate Research Branch of the Meteorological Service of Canada (MSC) has a long standing research program in the development of space-borne passive microwave SWE datasets for specific landscape regions (Walker and Goodison 2000). The current operational suite of MSC algorithms include unique empirically derived equations to estimate SWE for open environments, and coniferous, deciduous, and sparse classes of forest cover. These regional algorithm development efforts have led to climatological analysis of a passive microwave derived SWE time series for central North America (Derksen et al. 2004), and are used for climate model initialization and validation (MacKay and Derksen 2003). Weekly SWE maps

are also produced operationally at the MSC and distributed to water resource management agencies, hydropower companies, and weather forecast offices.[1]

Previous studies have illustrated the high degree of intra- and inter-annual variability in the spatial extent of terrestrial snow cover, and trends through time, using snow charts derived from optical satellite data (Gutzler and Rosen 1992), space-borne passive microwave data (Armstrong and Brodzik 2001), and conventional measurements (Brown 2000). Some attention has also been focused on trends and variability in hydrologically significant snow cover variables such as depth and SWE (Cayan 1996; Serreze et al. 1999), although these datasets are typically derived from *in situ* point observations.

Efforts to map snow cover using passive microwave data have enabled the development of a 24 year (1978 to 2002) spatially continuous characterization of SWE. These data sets provide an exceptional opportunity to investigate the variability and stability in temporal patterns of SWE. Composite SWE patterns at different temporal resolutions and time periods capture different characteristics of the seasonal snow conditions. For instance, late winter average SWE values (February, March, or April depending on location) are often used as an indication of maximum seasonal snow extent (i.e., McCabe and Legates 1995).

Twenty-four years of spatially extensive SWE values provide a unique opportunity to add to the understanding of spatial variability in climate perturbations through time. The goal of this study is to explore spatially the temporal variability in mean February SWE values derived using the land cover sensitive MSC algorithm suite applied to non-mountainous regions of western Canada (Derksen et al. 2003a,b). The February time period was selected to provide an annual perspective on SWE when North American snow extent is expected to be at maximum. Several questions are considered to aid the investigation of temporal trends in SWE values.

(1) Are there spatial variations in the frequency with which annual February mean SWE values vary significantly from mean February SWE values for all 24 years?
(2) Is there a spatial pattern in the cumulative variability between annual February mean SWE values and mean February SWE values for all 24 years?
(3) Does the spatial pattern of temporal variability in SWE values change through time?

For locations identified as having interesting spatial patterns in the temporal variability of SWE values the characteristics of vegetation were assessed at two spatial scales: at a coarse scale ecozone data were used for comparison while satellite derived land cover data provided a means for finer scale investigations.

2 Study area and data

2.1 Passive microwave derived SWE dataset

Space-borne passive microwave data are appropriate for regional monitoring of snow cover due to characteristics such as all-weather imaging, a wide swath width with frequent overpass times, and a long time series (1978 – present). Perhaps most significantly, the scattering influence of dry snow cover allows the estimation of SWE, a variable that cannot be derived from optical space-borne imagery. The retrieval of SWE information from passive microwave brightness temperatures is theoretically straightforward: as the depth and density of snow

[1] URL: http:// www.socc.ca/snow/snow_current_e.cfm.

Table 1 Comparison of SMMR and SSM/I sensors

	SMMR	SSM/I
Platform	NIMBUS-7	DMSP F8; F11; F13
Time series	Oct. 26 1978 – Aug. 20 1987	July 9 1987 – Present
Channels (GHz) and footprint (km)	6.6:148 × 95	19.35:69 × 43
	10.69:91 × 59	22.345:60 × 40
	18:55 × 41	37:37 × 28
	21:46 × 30	85.5:15 × 13
	37:27 × 18	
Cross/along track interval	14 × 14 to 56 × 28 km	25 × 25 km (85.5 = 12.5 × 12.5 km)
Polarization	V and H, all channels	V and H, except 22 GHz (V only)
Viewing Angle	50.2°	53.1°
Data acquisition	Every other day	Daily
Swath width	780 km	1400 km
Approximate	Ascending – noon equatorial crossing	F8: Ascending – 0600 equatorial crossing
Orbital timing	Descending – midnight equatorial crossing	F11/13: Ascending – 1800 equatorial crossing

increases, so too does the amount of volume scatter of naturally emitted microwave energy. Shorter wavelength energy (i.e. 37 GHz) is more readily scattered by snow grains than longer wavelength energy (i.e. 19 GHz), so the difference in scatter between these two satellite-measured frequencies can be exploited to estimate SWE, which is reported in mm. In reality, the relationships between snow depth, density, and microwave scatter are complicated by the physical structure of the snowpack (e.g., ice lenses, the presence of liquid water, and snow grain size variability) and the microwave emission and scattering characteristics of overlying vegetation. The imaging footprint for space-borne passive microwave data is large (grid cell dimensions of 25 km) so these complicating factors are compounded by considerable within-grid cell variability in snowpack structure and vegetative cover.

The period of available multi-frequency space-borne passive microwave brightness temperatures includes SMMR data from 1978 through 1987 and SSM/I data from 1987 to the present. The SMMR and SSM/I data are available in a common gridded format (the Equal Area Scalable Earth Grid - EASE-Grid; see Armstrong and Brodzik 1995) from the National Snow and Ice Data Center (Knowles et al. 1999; Armstrong et al. 1993). The sensors have slightly different spatial, temporal, and radiometric characteristics (Table 1) that impact the continuity and consistency of cross-platform brightness temperatures and derived geophysical variables. When unadjusted EASE-Grid brightness temperatures are utilized, SWE and snow cover extent retrievals during SMMR seasons are systematically and significantly lower than retrievals during SSM/I seasons (Derksen et al. 2003a). Derksen and Walker (2003) derived new regression-based coefficients with sensitivity to overpass time using co-located brightness temperatures over terrestrial surfaces of central North America from the August 1987 period of overlap between the SMMR and the first SSM/I onboard the U.S. Defence Meteorological Satellite Program (DMSP) F-8 satellite. This procedure adjusted SMMR brightness temperatures to an SSM/I F-8 baseline, and removed the bias in SWE retrievals (Derksen et al. 2004).

In Canada, algorithm development for SWE retrieval from space-borne passive microwave brightness temperatures initially focused on the open, generally non-forested environment of the Canadian prairies (Goodison and Walker 1995; Walker and Goodison 2000). More recently, general algorithms have been produced for boreal forest cover (Goita et al. 2003). The open prairie algorithm is based on the brightness temperature gradient between the 37 and 19 GHz (18 GHz with SMMR) vertically polarized channels [(37 V–19 V)/18], while the three forest algorithms are based on the brightness temperature difference of these same channels (37 V-19 V). The resulting suite of land cover sensitive SWE retrieval algorithms can be applied to both SMMR and SSM/I brightness temperatures, with per-grid cell SWE estimates produced as the sum of the SWE values obtained from each land cover algorithm weighted by the percentage land cover type (F) within each grid cell:

$$\mathrm{SWE} = F_D \mathrm{SWE}_D + F_C \mathrm{SWE}_C + F_S \mathrm{SWE}_S + F_O \mathrm{SWE}_O \quad (1)$$

where *D* represents deciduous forest, *C* coniferous forest, *S* sparse forest, and *O* open Prairie environments. Grid cell land cover fractions are determined from the International Geosphere – Biosphere Programme (IGBP) 1 km global land cover classification (Loveland et al. 2000), resampled to the EASE-Grid by NSIDC. The 17 IGBP classes are reduced to the four algorithm classes (open, coniferous, deciduous, and sparse forest). Full details on algorithm development and initial validation are provided in Goodison and Walker (1995) and Goita et al. (2003).

Evaluation of SWE retrievals at the coarse resolution of passive microwave data is complicated by within pixel heterogeneity in vegetation and snow cover properties. Point measurements of snow depth from climate observing stations are of limited utility because of sparse observing networks and difficulty in comparing point measurements to integrate retrievals within a 625 km^2 area (of the 25 $\times$ 25 km pixel). Through a combination of field studies and use of historical climate data, evaluation studies have shown that SWE retrievals are typically within $\pm$20% of surface observations in the open prairies. Consistent underestimation of SWE is a problem in heavily forested areas due to the complex impact of dense vegetation on microwave emission and scatter (Walker and Silis 2002; Derksen et al. 2003b). Regional snow surveys conducted recently across the boreal forest environment of northern Manitoba identified strong agreement in SWE spatial distribution, with mean underestimation of 17% in February 2004 (Derksen et al. 2005). This value increased to nearly 30% during the heavier snow season sampled during the most recent field season of February 2005. Evaluation of the open environments algorithm in tundra areas has been limited (see Woo 1998; Wang et al. 2005). Challenges include wind redistribution across the tundra (the removal of snow from flat and exposed areas and the deposition of deep drifts along lee slopes of topographical relief such as river valleys, eskers, and lake shorelines), and potentially high sublimation loss (Pomeroy and Li 2000). A comparison of passive microwave derived SWE with Canadian Regional Climate Model simulations and station precipitation data by MacKay and Derksen (2003) showed strong inter-dataset agreement from December through February, but passive microwave SWE underestimation in March. A regional snow survey completed across the open tundra of northern Manitoba during the 2003/04 winter (Derksen et al. 2005) suggests that SWE retrievals in this environment are representative of open, low-relief areas, but underestimate SWE by approximately 40% when deep drifts are included in per-grid cell computations of *in situ* SWE.

While research into a tundra-specific SWE algorithm is on-going, the collective assessments of algorithm performance completed to date allow SWE retrievals for the non-mountainous regions of the interior of North America to be examined with confidence (see

Fig. 1 The study area includes the non-mountainous portion of Ontario and Western Canada. Analysis is restricted to an area for which algorithm development and evaluation efforts are completed or on-going, and for which land cover and ecozone data were available

Figure 1). In this study, analysis is constrained to an area where algorithm performance has been demonstrated to be suitable for climatological analysis (Derksen et al. 2003a, b). Analysis was also limited to Canada due to the availability of detailed land cover and ecozone data.

All the satellite brightness temperature frequencies have grid cell dimensions of 25 km by 25 km, although the microwave emission is measured from larger, elliptical fields of view and resampled (see Armstrong and Brodzik 1995, for a complete description of the EASE-Grid resampling procedure). Two orbits of data were acquired daily (ascending and descending overpasses), although the SMMR was deactivated every other day as a power saving measure. For the present study, mean February SWE patterns were derived for a 24 year time period (1978 to 2002). February values generate a consistent representation of approximately maximum snow cover conditions in all years.

2.2 Ecozone and land cover data

Landscape characteristics play an important role in the catchment, redistribution, and physical properties of snow cover, and influence the microwave properties of the surface. Two scales of land cover information were utilized in this study, to provide an interpretive context to the spatial-temporal analysis of the SWE time series. An ecosystem is a unit of nature that is characterized by living and non-living elements, and the relationship between them (Wiken et al. 1996). In Canada, general ecosystems are mapped as ecozones and the Canadian terrestrial ecozones (Table 2) provide a basis for regional management. In this study we assess the impact of vegetation, in a broad sense, on the temporal variability of SWE values by relating interesting spatial-temporal patterns identified in the data to ecozones.

Table 2 List of ecozones and land cover classes. Ecozone abbreviations in bold type are used in this study

Ecozone information		
Ecozone	Vegetation description	Land cover information class descriptions
Arctic Cordillera (AC)	Mainly unvegetated; some shrub-herb tundra	Broadleaved Deciduous Forest – closed canopy
Northern Arctic (**NA**)	Herb-lichen tundra	Needleleaved Evergreen Forest – closed canopy
Southern Arctic (**SA**)	Shrub-herb tundra	Needleleaved Evergreen Forest – open canopy
Taiga Plains (**TP**)	Open to closed mixed evergreen-deciduous forest	Needleleaved Mixed Forest – closed canopy
Taiga Shield (**TS**)	Open evergreen-deciduous trees; some lichen-shrub tundra	Mixed Broadleaved or Needleleaved Forest – closed canopy
Taiga Cordillera (TC)	Shrub-herb-moss-lichen tundra	Mixed Broadleaved or Needleleaved Forest – open canopy
Hudson Plains (**HP**)	Wetland; some herb-moss-lichen tundra, evergreen forest	Broadleaved Evergreen Shrubland – closed canopy
Boreal Plains (**BP**)	Mixed evergreen-deciduous forest	Broadleaved Deciduous Shrubland – open canopy
Boreal Shield (**BS**)	Evergreen forest, mixed evergreen-deciduous forest	Needleleaved Evergreen Shrubland – open canopy
Boreal Cordillera (BC)	Largely evergreen forest; some tundra, open woodland	Mixed Broadleaved and Needleleaved Dwarf-Shrubland – open canopy
Pacific Maritime (PM)	Coastal evergreen forest	Grassland
Montane Cordillera (MC)	Evergreen forest, alpine tundra, interior grassland	Grassland with sparse tree layer
Prairies (**P**)	Grass; scattered deciduous forest	Grassland with sparse shrub layer
Atlantic Maritime (AM)	Mixed deciduous-evergreen forest	Dwarf sparse shrub layer
Mixedwood Plains (MP)	Mixed deciduous-evergreen forest	Cropland
		Cropland and Shrubland/Woodland
		Needleleaved Evergreen Forest – open canopy – lichen understory
		Unconsolidated material sparse vegetation
		Urban
		Consolidated rock sparse vegetation
		Water
		Burnt
		Snow and Ice
		Wetlands
		Herbaceous Wetlands
		Broadleaved Evergreen Forest – open canopy

At a finer scale, the relationship between temporal patterns in SWE and vegetation is investigated using land cover. Land cover data for year 2000 were generated as part of the Global Land Cover 2000 Project, which produced the Land Cover Map of North and Central America (Latifovic et al. 2004). Land cover data were generated from imagery with a 1 km spatial resolution, captured by the VEGETATION instrument on board the SPOT 4 satellite. When compared to three other global land cover classifications (produced by the US Geological Survey, Maryland University, and Boston University) the Land Cover Map of North and Central America had approximately 80% pixel correspondence, and the majority of disagreement occurred in transitions zones (Latifovic et al. 2004), as is typical with coarse spatial resolution large area land cover maps (Wulder et al. 2004). For full details on the methods used to generate this land cover map, refer to Latifovic et al. (2004). The land cover classes used in this study are provided in Table 2.

3 Analytical approach and results

Three spatial analysis approaches were used to investigate variability and stability in the spatial-temporal pattern of SWE values through the 24-year data record. Collectively, these analysis techniques allowed complementary questions to be investigated, and the nature of SWE over space and time to be explored.

3.1 Characterizing SWE extremes via mean comparisons

As an initial point of analysis, the frequency with which annual SWE values were significantly different from the average was investigated for the full time series. On a grid cell by grid cell basis, mean February SWE values from 1978 to 2002 were generated (Mean-All), and compared to the 24 individual mean Z-score February SWE values. For individual pixels, the frequency distributions of SWE values used to calculate Mean-All were approximately normal. Mean-All summarizes the general temporal trend in SWE values. Therefore, annual SWE means are assessed relative to general trends by computing the probability that annual values fall within a normal distribution having a mean and variance equivalent to Mean-All. This was done using a standard normal transformation, or Z-score conversion. If Z-scores were outside ± 1.96 (95% confidence level), annual values were considered significantly different than the time series mean. For each grid cell, the number of years having significant positive or negative Z-scores were computed and mapped.

Variability of annual SWE values, relative to the Mean-All, can be seen in Figure 2a. The maximum number of years that an individual pixel was significantly high or low was four (out of a possible 24), however most locations were only significantly high or low in a single year.

When variability is characterized using significantly positive Z-scores (Figure 2b), highly variable locations occur primarily in the north and south of the study area, in the Southern Arctic (SA) and Prairie (P) ecozones. In contrast, when only significantly negative Z-scores are plotted (Figure 2c), the most variable locations are found in the Taiga Plains (TP), Taiga Shield (TS), and Boreal Shield (BS) ecozones. To assist the interpretation of these results, it is helpful to examine the mean February SWE pattern, shown in Figure 2d. The dominant feature in this pattern is the zone of high SWE values that extend across the boreal forest from Northern Ontario to the northwest through northern Manitoba and the Northwest Territories. Statistically significant positive SWE departures do not occur through this region (Figure 2b). A possible contributing factor to this finding is that the theoretical limit for SWE retrievals

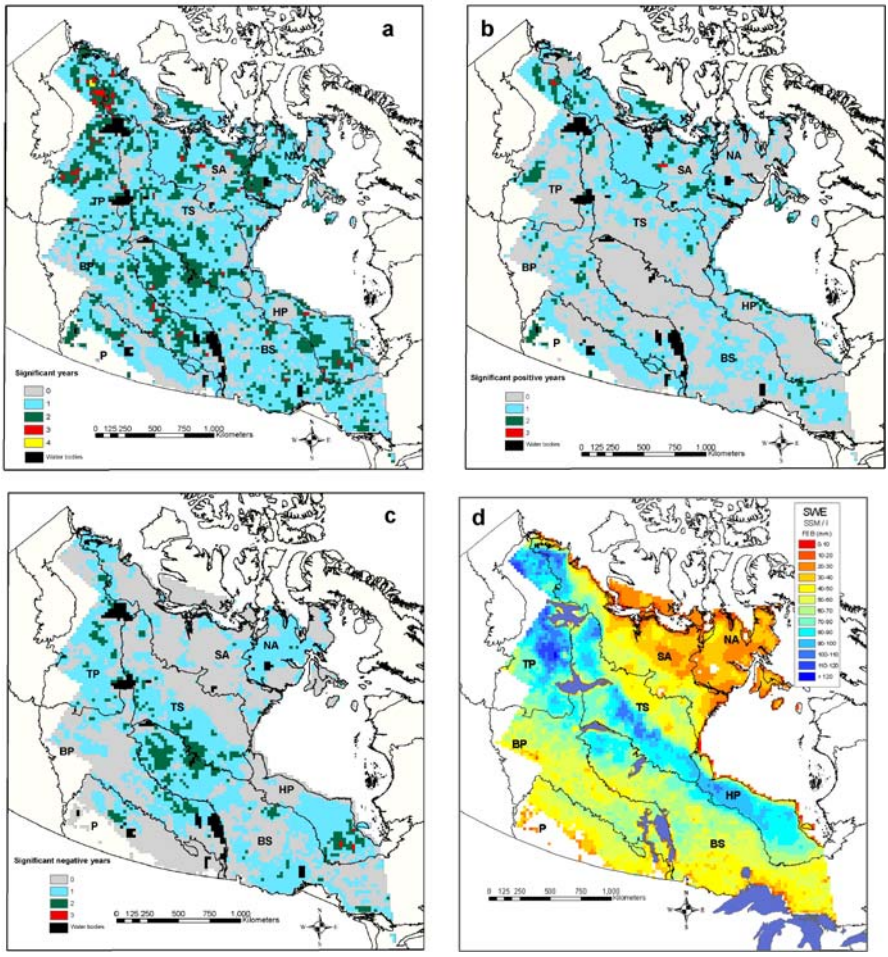

Fig. 2 (a) The number of years seasonal SWE values are statistically different than the Mean-All. (b) The number of years the seasonal SWE value is statistically *higher* than Mean-All. (c) The number of years the seasonal SWE value is statistically *lower* than Mean-All. Total number of years compared to Mean-All is 24. (d) Passive microwave derived average monthly SWE for February 1979–2002

from algorithms that exploit the brightness temperature gradient technique is approximately 120–130 mm (Armstrong et al. 1993; De Seve et al. 1997), which is also the mean retrieved SWE value across this region in February. No significant positive departures will be found if retrievals over this value cannot physically be derived. While no significant positive departures were isolated for the region of highest SWE retrievals, it is interesting that the Northern Arctic (NA) ecozone, which has generally low SWE estimates, also has no positive SWE departures.

3.2 Characterizing variability and stability via cumulative differences

The first analysis approach isolated the temporal frequency of extreme February SWE values relative to the time series mean, yet the amount of variability was not identified. The spatial

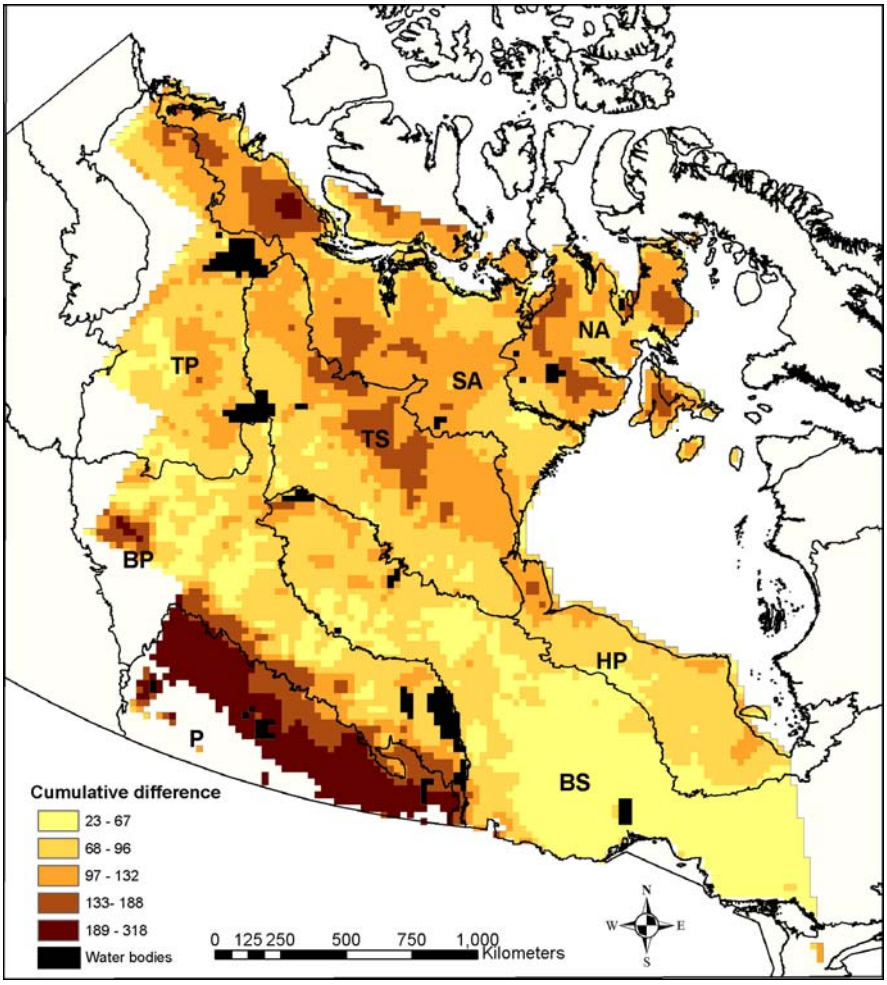

Fig. 3 Absolute cumulative differences between SWE values in each of the 24 years and Mean-All

patterns of temporal variability and stability in SWE were characterized using the sum of the absolute cumulative difference, hereafter referred to as cumulative difference, between February mean SWE values and Mean-All. This measure provides an indication of how variable a location is relative to other regions of the study area, but is of limited use when commenting on the nature of the variability. Values with large cumulative differences could have moderate variations relative to the mean in many years, or have large variations in a few years. However, locations with low variability are likely to have small differences relative to Mean-All in every year.

The cumulative difference between average February SWE values and Mean-All is shown in Figure 3. Strong cumulative differences were calculated over the Prairies with an abrupt transition to the Boreal Plain (BP), where low cumulative differences over the boreal forest were observed. Variable cumulative differences were computed over the Open Tundra. The Canadian prairies are clearly the region of maximum SWE variability: statistics derived from

Table 3 Summary of the distribution of cumulative differences between each year and Mean-All (CV = coefficient of variation)

Ecozone	Mean	Median	CV	Min	Max	*n*
Northern arctic	114.7	113.1	0.24	47.5	242.4	2124
Southern arctic	109.0	107.7	0.23	47.3	230.3	1239
Taiga plains	85.5	84.2	0.23	29.8	155.2	982
Taiga shield	99.5	96.0	0.25	45.9	166.4	1209
Boreal shield	60.7	58.0	0.33	23.0	183.5	1838
Boreal plains	89.8	78.6	0.44	26.3	260.9	1131
Prairies	200.5	210.3	0.23	53.5	318.3	538
Hudson plain	78.3	76.3	0.22	36.7	143.5	578

the frequency distributions of cumulative differences in each ecozone (Table 3) shows the Prairies and ecozones north of the tree line had the highest average variability, whereas the Boreal Shield had the lowest variability (Table 3).

As cumulative variability over the western Taiga Shield (TS) and Prairie (P) regions was markedly different, SWE frequency distributions of cumulative differences for each land cover class (representing at least 1% of the ecozone) were compared to the frequency distribution of all cumulative differences within the ecozone (Figures 4 and 5). When the frequency distributions diverge, spatial-temporal trends in SWE variation, associated with the individual land cover class, are different from the ecozone trend. The Prairie ecozone had much higher cumulative variability than the Western Taiga Shield. Lower variability in the Western Taiga Shield is likely the result of a greater proportion of forested land cover. In both ecozones, non-treed land cover classes are generally more variable than treed classes. This is most evident in the Prairies, where the modal cumulative variability for closed forest classes is shifted downwards, clearly having more low values than the complete ecozone (Figure 5: see needle leaved forest closed versus needle leaved forest open). As forested regions make up such a small proportion of the Prairie ecozone, this impact is limited across this region, but may have a more profound effect across the largely forested ecozones.

3.3 Characterizing temporal variability in patterns

For a third approach to characterizing spatial-temporal patterns in SWE, variability and stability was investigated through time. The goal of this analysis was to determine if the spatial pattern of variability in SWE values changed through time, relative to general trends. Annual data were separated into three groups: 1979 to 1986 (T_1), 1987 to 1994 (T_2), and 1995 to 2002 (T_3). For each 8-year period, differences between Mean-All and SWE values in individual years were calculated and summed. The spatial patterns of cumulative difference in SWE values are shown for each time period in Figure 6.

The spatial pattern of cumulative differences changes through time. High cumulative differences in SWE value are dispersed throughout the study area in T_1. In T_2 and T_3 variability is increasingly spatially restricted to the northern and Prairie ecozones. Ecozone summaries of cumulative differences provide additional insight into this visual interpretation (Table 4). For all ecozones, except the Prairies and Northern Arctic, the largest amount of variability occurs in T_1 and the least in T_2, with T_3 having an intermediate amount of variability. The Prairies are consistently the most variable ecozone, and have the highest cumulative variability in T_3 and the lowest variability in T_2. The Northern Arctic has the highest variability in T_2 and the lowest in T_3.

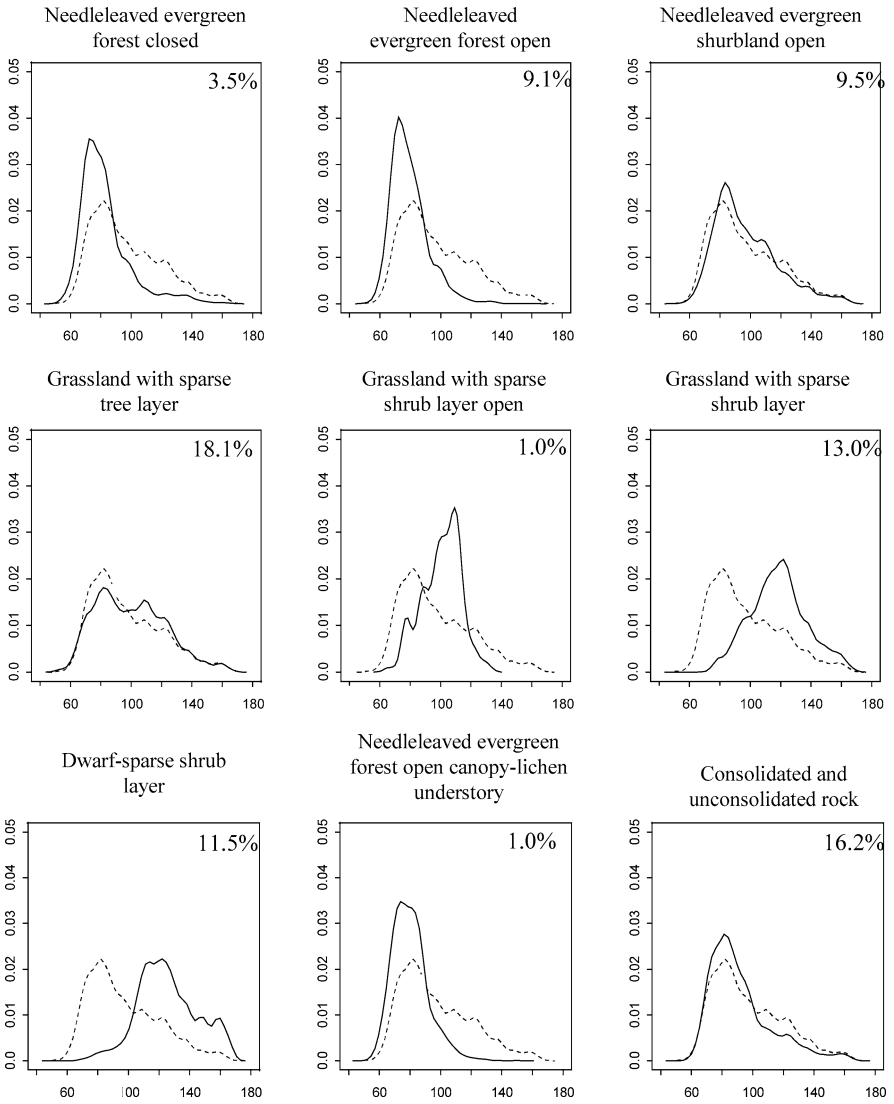

Fig. 4 For the West Taiga Shield ecozone a comparison of the overall distribution of absolute cumulative differences (dotted line) with the distribution in each land cover classes. Percent values reflect the percentage of the ecozone represented by each land cover class. Only land cover classes representing at least 1% of the ecozone were considered

While general temporal variation in snow cover is not increasing (T_1 is the time period with the most variability), the spatial arrangement of highly variable locations has changed. This may indicate changes in the characteristics of synoptic scale climatological influences on snowfall and ablation events across the study area, and will be the focus of follow-on study. As a point of comparison, linear trend analysis of Prairie SWE values showed no linear trends both for the satellite era alone and when merged with 85 years of conventional measurements (Derksen et al. 2004).

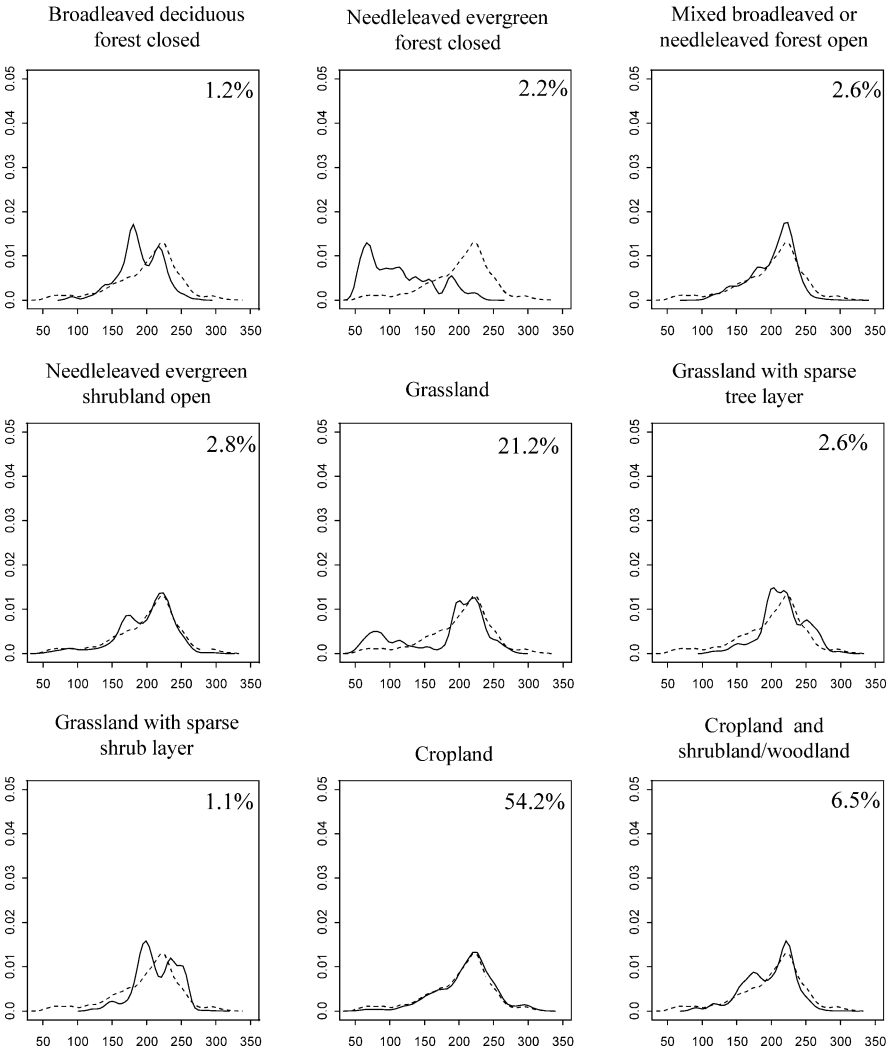

Fig. 5 For the Prairie ecozone a comparison of the overall distribution of absolute cumulative differences (dotted line) with the distribution in each land cover classes. Percent values reflect the percentage of the ecozone represented by each land cover class. Only land cover classes representing at least 1% of the ecozone were considered

4 Discussion and interpretation

There is a spatial component to temporal variability in mean February SWE values as discerned from the space-borne passive microwave data record. Spatial patterns appear, in part, to be related to vegetation. Histograms in Figures 4 and 5 indicate that forest cover impacts inter-annual variability in SWE retrievals. These results should be interpreted cautiously as uncertainty in passive microwave SWE retrievals is impacted by vegetation. In densely forested locations SWE values are systematically underestimated (Foster et al. 1991; Chang

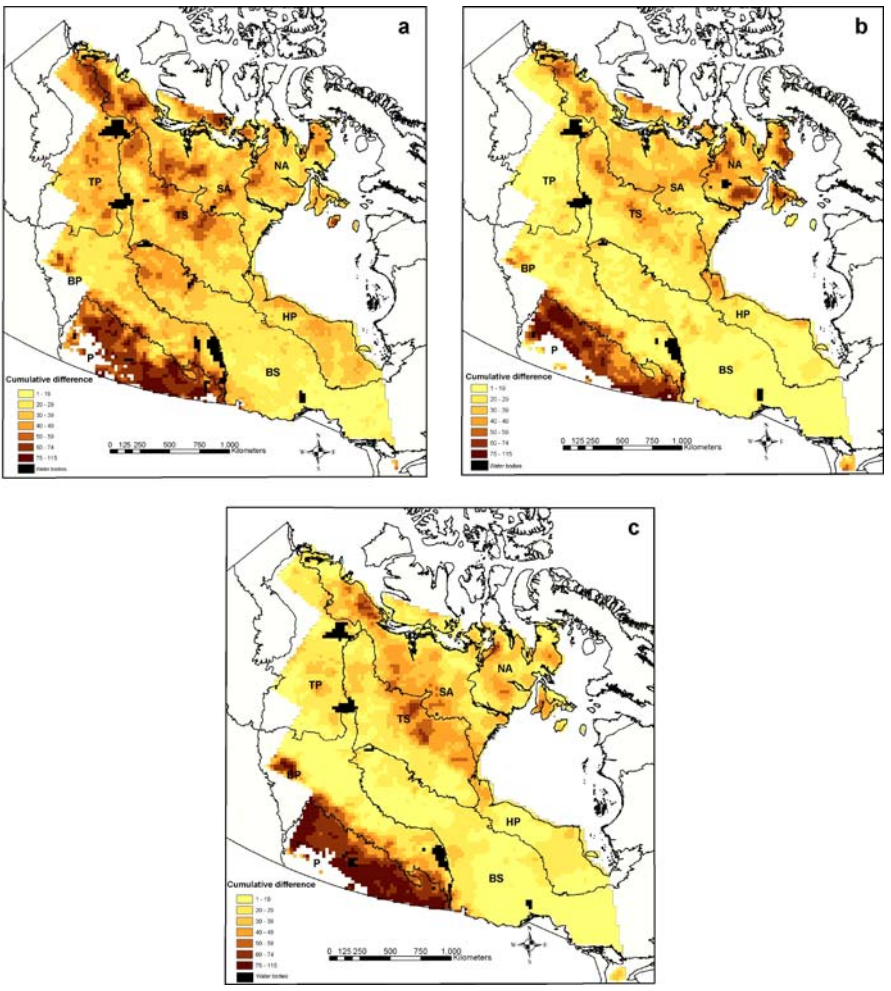

Fig. 6 Absolute cumulative differences between SWE values in (a) T_1 (1979–1986); (b) T_2 (1987–1994); and (c) T_3 (1995–2002) relative to Mean-All

et al. 1997), and in locations with open cover non-systematic inter-annual variability in algorithm performance as been noted (Derksen et al. 2003a).

There remains, however, evidence of temporal SWE variability over forested regions. Mean cumulative SWE differences for the forested ecozones are notably lower than for open environments (both Prairie and Arctic – Table 3); yet, it is important to note that cumulative differences for individual years were high in the forested Boreal Plains, relative to other ecozones (Table 4). This indicates that extreme SWE events in forested areas were captured by the passive microwave dataset; these large magnitude events are not consistent with inter-annual trends across the boreal forest as they are throughout the Prairies, and to a lesser degree, the open tundra. These results also indicate that through time extreme weather events may be occurring more consistently in the Prairies and Artic regions.

Different climatological forcing conditions are present across the boreal forest in winter relative to the southern Prairies. Snow and temperature sensitivity is acute across the Prairies

Table 4 Summary of the distribution of cumulative differences between each 8-yr segment and Mean-all

Ecozone	Mean	Median	CV	Min	Max	*n*
		T_1				
Northern arctic	35.6	34.3	0.35	5.8	83.5	2224
Southern arctic	37.5	35.7	0.33	10.4	79.4	1249
Taiga plains	38.0	36.7	0.27	14.0	83.2	983
Taiga shield	35.3	33.3	0.30	10.3	65.4	1209
Boreal shield	23.9	22.1	0.39	5.0	65.9	1842
Boreal plains	31.6	29.5	0.37	6.5	76.7	1134
Prairies	62.4	64.3	0.24	14.7	103.0	651
Hudson plain	30.1	30.0	0.22	10.6	47.6	578
		T_2				
Northern arctic	39.5	38.7	0.33	5.6	98.9	2189
Southern arctic	32.5	32.5	0.28	8.4	65.2	1245
Taiga plains	18.7	17.6	0.36	5.3	53.7	991
Taiga shield	27.7	26.5	0.33	8.9	57.0	1213
Boreal shield	15.5	14.6	0.44	3.5	51.6	1851
Boreal plains	24.4	21.8	0.48	5.1	71.7	1147
Prairies	61.0	62.7	0.32	8.6	108.9	584
Hudson plain	20.9	19.1	0.39	2.5	52.8	578
		T_3				
Northern arctic	33.2	31.9	0.35	8.4	75.5	2237
Southern arctic	34.7	34.9	0.31	5.6	67.6	1244
Taiga plains	22.6	22.4	0.34	3.8	52.2	989
Taiga shield	30.6	27.2	0.40	11.1	70.7	1214
Boreal shield	17.1	16.4	0.40	4.6	64.0	1856
Boreal plains	27.8	22.1	0.67	4.9	110.7	1148
Prairies	72.3	74.0	0.25	11.8	111.6	624
Hudson plain	21.1	19.8	0.31	10.1	49.8	578

CV = coefficient of variation

(Karl et al. 1993) as temperatures can fluctuate near zero during the onset and melt of the snow cover season, and also during mid-winter melt events. The mid-latitude jet controls temperature and moisture advection, and inter-annual variability in jet dynamics can dictate precipitation phase, amount, and distribution. At higher latitudes, the Arctic jet influences lee trough formation with associated frontogenesis and precipitation. The sensitivity of snow cover to temperature is reduced compared to more southerly latitudes as temperatures remain well below freezing during the months examined in this study. Given the high degree of inter-annual variability SWE distribution and magnitude across the Canadian Prairies, the potential existence of a consistent SWE zone across the northern boreal forest apparently resistant to inter-annual climatic variability over the past 24 years is intriguing in the context of the sensitivity of snow cover to climate variability and change.

5 Conclusions

SWE datasets derived from passive microwave data provide a temporally extensive and spatially continuous perspective on a variable that is historically measured at discrete locations. In this study, we exploit these characteristics to gain a multi-temporal and spatial perspective on SWE variability across much of interior Canada through the satellite era. The results presented in this study have use for other applications, such as linking winter snow cover

with Prairie drought activity (Liu et al. 2004) and trends and variability in summer fire risk (Gillett et al. 2004).

Regarding the questions posited to define this research, we found that,

- There are spatial variations in the frequency with which annual February mean SWE values vary from mean February SWE values averaged over all 24 years. Considering these 24 year vectors, a statistically significant variability from the mean vector value can be found up to four times. Spatially, vectors of highest variability are found most frequently in the northern ecozones, although isolated zones of high variability occur in more southerly locations.
- There are spatial patterns in the cumulative variability between annual February mean SWE values and mean February SWE values for all 24 years. High cumulative variability tends to occur in the Prairie and northern ecozones.
- The spatial patterns of temporal variability in SWE values do change through time. These changes in spatial pattern of temporal variability, as found through the comparison of three eight year time periods, illustrate a dispersion of variability in the initial time period that is not present in the later time periods. High values for cumulative variability are becoming spatially clustered over time, with the greatest variability in snow cover found in northern and Prairie ecozones.

The results from this study also demonstrate that there is a relationship between temporal variability in SWE values and vegetation and that the spatial structure in the temporal variability of SWE values is changing through time. Although the 24-year time series provides a unique opportunity to investigate such issues, the strength of these relationships is difficult to ascertain due to uncertainty associated with the retrieved SWE values. Additional insights will be gained through future integration of results with indicators of low-frequency atmospheric circulation. For example, a quasi-decadal shift in atmospheric circulation was noted immediately before the satellite passive microwave time series began (1977), and occurred again in 1989 (Watanabe and Nitta 1999). Strong ENSO events are also present within the passive microwave data record.

Barring a series of sensor failures, the passive microwave time series will continue uninterrupted into the future, both with continuing SSM/I data acquisition, and the 2002 launch of new generation sensors such as the Advanced Microwave Scanning Radiometer (AMSR-E). This time series will continue to be an important resource for identifying spatial and temporal trends in SWE for climatological, hydrological, and numerical modelling studies.

Acknowledgements The EASE-Grid brightness temperature data were obtained from the EOSDIS National Snow and Ice Data Center Distributed Active Archive Center (NSIDC DAAC), University of Colorado at Boulder. The availability of the SPOT VGT land cover product produced by Canada Centre for Remote Sensing (Natural Resources Canada) and the United States Geological Survey is appreciated.

References

Armstrong R, Brodzik M (1995) An earth-gridded SSM/I data set for cryospheric studies and global change monitoring. Advanced Space Research 16(10):10155–10163

Armstrong R, Brodzik M (2001) Recent Northern Hemisphere snow extent: a comparison of data derived from visible and microwave satellite sensors. Geophysical Research Letters 28(19):3673–3676

Armstrong R, Chang A, Rango A, Josberger E (1993) Snow depths and grain-size relationships with relevance for passive microwave studies. Annals of Glaciology 17:171–176

Armstrong RL, Knowles KW, Brodzik MJ, Hardman MA (1994–2002) DMSP SSM/I Pathfinder daily EASE-Grid brightness temperatures. Boulder, CO: National snow and ice data center. Digital media and CD-ROM

Brown R (2000) Northern Hemisphere snow cover variability and change, 1915–1997. Journal of Climate 13:2339–2355

Cayan D (1996) Interannual climate variability and snowpack in the Western United States. Journal of Climate 9(5):928–948

Chang A, Foster J, Hall D (1990) Satellite sensor estimates of northern hemisphere snow volume. International Journal of Remote Sensing 11(1):167–171

Chang A, Foster J, Hall D, Goodison B, Walker A, Metcalfe J, Harby A (1997) Snow parameters derived from microwave measurements during the BOREAS winter field campaign. Journal of Geophysical Research 102(D24):29 663–29 671

Cohen J, Entekhabi D (2001) The influence of snow cover on Northern Hemisphere climate variability. Atmosphere-Ocean 39(1):35–53

De Seve D, Bernier M, Fortin J-P, Walker A (1997) Preliminary analysis of snow microwave radiometry using the SSM/I passive-microwave data: the case of La Grande River watershed (Quebec). Annals of Glaciology 25:353–361

Derksen C, Brown R, Walker A (2004) Merging conventional (1915–1992) and passive microwave (1978–2002) estimates of snow extent and water equivalent over central North America. Journal of Hydrometeorology 5(5):850–861

Derksen C, Walker A (2003) Identification of systematic bias in the cross-platform (SMMR and SSM/I) EASE-Grid brightness temperature time series. IEEE Transactions on Geoscience and Remote Sensing 41(4):910–915

Derksen C, Walker A, LeDrew E, Goodison B (2003a) Combining SMMR and SSM/I data for time series analysis of central North American snow water equivalent. Journal of Hydrometeorology 4(2):304–316

Derksen C, Walker A, Goodison B (2003b) A comparison of 18 winter seasons of *in situ* and passive microwave derived snow water equivalent estimates in Western Canada. Remote Sensing of Environment 88(3):271–282

Derksen C, Walker A, Goodison B (2005) Evaluation of passive microwave snow water equivalent retrievals across the boreal forest/tundra transition of western Canada. Remote Sensing of Environment 96:315–327

Foster J, Chang A, Hall D, Rango A (1991) Derivation of snow water equivalent in boreal forests using microwave radiometry. Arctic 44:147–152

Gillett N, Weaver A, Zwiers F, Flannigan M (2004) Detecting the effect of climate change on Canadian forest fires. Geophysical Research Letters 31(18):L18211

Goita K, Walker A, Goodison B (2003) Algorithm development for the estimation of snow water equivalent in the boreal forest using passive microwave data. International Journal of Remote Sensing 24(5):1097–1102

Gong G, Entekhabi D, Cohen J (2003) Relative impacts of Siberian and North American snow anomalies on the winter Arctic Oscillation. Geophysical Research Letters 30(16):1848–1851

Goodison B, Walker A (1995) Canadian development and use of snow cover information from passive microwave satellite data. In: Choudhury B, Kerr Y, Njoku, E. and Pampaloni, P. (eds.). Passive Microwave Remote Sensing of Land-Atmosphere Interactions. VSP BV, Utrecht, Netherlands, pp. 245–262

Grody N, Basist A (1996) Global identification of snowcover using SSM/I measurements. IEEE Transactions on Geosciences and Remote Sensing 34(1):237–249

Gutzler D, Rosen R (1992) Interannual variability of wintertime snow cover across the Northern Hemisphere. Journal of Climate 5:1441–1447

Hall D, Riggs G, Salomonson V, DiGirolamo N, Bayr K (2002) MODIS snow-cover products. Remote Sensing of Environment 83:181–194

Josberger E, Mognard N, Lind B, Matthews R, Carroll T (1998) Snowpack water-equivalent estimates from satellite and aircraft remote-sensing measurements of the Red River basin. north-central U.S.A, Annals of Glaciology. 26:119–124

Karl T, Groisman P, Knight R, Heim R (1993), Recent variations of snow cover and snowfall in North America and their relation to precipitation and temperature variations. Journal of Climate 6:1327–1344

Kelly R, Chang A, Tsang L, Foster J (2003) A prototype AMSR-E global snow area and snow depth algorithm. IEEE Transactions on Geoscience and Remote Sensing 41(2):230–242

Knowles KW, Njoku EG, Armstrong RL, Brodzik MJ (1999) Nimbus-7 SMMR Pathfinder daily EASE-Grid brightness temperatures. Boulder, CO: National snow and ice data center. Digital media and CD-ROM

Latifovic R, Zhu Z, Cihlar J, Giri C, Olthof I (2004) Land cover of north America – Global Land Cover 2000. Remote Sensing of Environment 89:116–127

Liu J, Stewart R, Szeto K (2004) Moisture transport and other hydrometeorological features associated with the severe 2000/01 drought over the western and central Canadian prairies. Journal of Climate 17:305–319

Loveland T, Reed B, Brown J, Ohlen D, Zhu Z, Yang L, Merchant J (2000) Development of a global land cover characteristics database and IGBP DISCover from 1 km AVHRR data. International Journal of Remote Sensing 21(6 & 7):1303–1330

MacKay M, Derksen C (2003) Regional Snowpack Modelling over Canadian Landscapes. Northern Basins Symposium August 2003 Greenland, pp 7

McCabe G, Legates D (1995) Relationships between 700 hPa height anomalies and April snow pack accumulations in the Western USA. International Journal of Climatology 15:517–530

Pomeroy J, Li L (2000) Prairie and Arctic areal snow cover mass balance using a blowing snow model. Journal of Geophysical Research 105(D21):26619–26634

Pulliainen J, Hallikainen M (2001) Retrieval of regional snow water equivalent from space-borne passive microwave observations. Remote Sensing of Environment 75:76–85

Serreze M, Clark M, Armstrong R, McGinnis D, Pulwarty R (1999) Characteristics of the western United States snowpack from snowpack telemetry (SNOTEL) data. Water Resources Research 35(7):2145–2160

Serreze M, Walsh J, Chapin III F, Osterkamp T, Dyurgerov M, Romanosky V, Oechel W, Morison J, Zhang T, Barry R (2000) Observational evidence of recent change in the northern high-latitude environment. Climatic Change 46:159–207

Tait A (1998) Estimation of snow water equivalent using passive microwave radiation data. Remote Sensing of Environment 64:286–291

Walker A, Goodison B (2000) Challenges in determining snow water equivalent over Canada using microwave radiometry. In Proceedings, International Geoscience and Remote Sensing Symposium. Honolulu, July, 2000, pp 1551–1554

Walker A, Silis A (2002) Snow cover variations over the Mackenzie river basin from SSM/I passive microwave satellite data. Annals of Glaciology 34:8–14

Watanabe M, Nitta T (1999) Decadel changes in the atmospheric circulation and associated surface climate variations in the Northern Hemisphere Winter. Journal of Climate 12:494–510

Wiken E, Gauthier D, Marshall I, Lawton K, Hirvonen H (1996) A perspective on Canada's Ecosystems: an overview of the Terrestrial and Marine Ecozones. Occasional paper N. 14. Canadian Council on Ecological Areas, Ottawa, Ont. pp 95

Wang L, Sharp M, Brown R, Derksen C, Rivard B (2005) Evaluation of spring snow covered area depletion in the Canadian Arctic from NOAA snow charts. Remote Sensing of Environment 95:453–463

Woo M-K (1998) Arctic snow cover information for hydrological investigations at various scales. Nordic Hydrology 29(4/5):245–266

WCRP (2002) CliC: Climate and Cryosphere Project, Science Plan. http://clic.npolar.no/introduction/science_plan.php [Accessed October 13, 2004]

Wulder M, Boots B, Seemann D, White J (2004) Map comparison using spatial autocorrelation: An example using AVHRR derived land cover of Canada. Canadian Journal of Remote Sensing 30(4):573–592